



Published in final edited form as:

Sci Transl Med. 2015 March 4; 7(277): 277ra29. doi:10.1126/scitranslmed.3010383.

A Synthetic Fibrin-Crosslinking Polymer for Modulating Clot Properties and Inducing Hemostasis

Leslie W.-G. Chan¹, Xu Wang², Hua Wei¹, Lilo D. Pozzo³, Nathan J. White^{2,*}, and Suzie H. Pun^{1,*}

¹Department of Bioengineering and Molecular Engineering and Sciences Institute, University of Washington, 3720 15th Avenue NE, Box 355061, Seattle, WA 98195, USA

²Department of Bioengineering and Molecular Engineering and Sciences Institute, University of Washington, 3720 15th Avenue NE, Box 355061, Seattle, WA 98195, USA

³Department of Chemical Engineering, University of Washington, Seattle, WA, 98195, USA

Abstract

Clotting factor replacement is the standard management of acute bleeding in congenital and acquired bleeding disorders. We present a synthetic approach to hemostasis using an engineered hemostatic polymer (PolySTAT) that circulates innocuously in the blood, identifies sites of vascular injury, and promotes clot formation to stop bleeding. PolySTAT induces hemostasis by crosslinking the fibrin matrix within clots, mimicking the function of the transglutaminase Factor XIII. Furthermore, synthetic PolySTAT binds specifically to fibrin monomers and is uniformly integrated into fibrin fibers during fibrin polymerization, resulting in a fortified, hybrid polymer network with enhanced resistance to enzymatic degradation. *In vivo* hemostatic activity was confirmed in a rat model of trauma and fluid resuscitation in which intravenous administration of

*To whom correspondence should be addressed: spun@uw.edu (S.H.P.); whiten4@uw.edu (N.J.W.).

Supplementary Materials

Materials and Methods

Fig. S1. TEG measurements for fibrinogen and plasmin titration study.

Fig. S2. In vitro comparison of PolySTAT to PolySCRAM and component controls.

Fig. S3. TEG measurements for hemodilutions.

Fig. S4. Prothrombin time in rat femoral artery injury models.

Fig. S5. Fibrinogen concentration in rat femoral artery injury models.

Fig. S6. Mean arterial pressure (MAP) in rat femoral artery injury models.

Fig. S7. Lactate concentration of rat femoral artery injury models.

Table S1. Comprehensive metabolic and hepatic function panel results for 1 hr, 1 day, and 1 week after PolySTAT injection in rats.

Table S2. Pharmacokinetic constants for PolySTAT

Table S3.. PolySTAT content in urine after tail-vein injection.

Movie S1. Lysis of control fibrin formed with PBS.

Movie S2. Lysis of control fibrin formed with PolySCRAM.

Movie S3. Lysis of PolySTAT-modified fibrin.

Movie S4. Lysis of hFXIIIa-crosslinked fibrin.

Author contributions: L.W.C, N.J.W., and S.H.P. conceived the idea of multivalent fibrin-targeted polymers for crosslinking fibrin matrices, designed experiments, analyzed results and wrote the manuscript. L.W.C. and H.W. synthesized the fibrin-crosslinking polymers. L.W.C. completed polymer characterization and in vitro evaluations. L.P. provided expertise on mechanical properties of gels. X.W. and L.W.C. refined the rat femoral artery injury model and completed in vivo testing of materials.

Competing interests: The University of Washington has applied for a patent for the discussed hemostatic materials with S.H.P., N.J.W., and L.W.C. listed as the inventors.

Data and materials availability: Materials used in PolySTAT synthesis are all available commercially.

PolySTAT improved survival by reducing blood loss and resuscitation fluid requirements. PolySTAT-induced fibrin crosslinking is a novel approach to hemostasis utilizing synthetic polymers for non-invasive modulation of clot architecture with potentially wide-ranging therapeutic applications.

Introduction

Bleeding is responsible for 30–40% of trauma-associated deaths and is the leading cause of death in the initial hours after injury (1). The formation of stable blood clots, or hemostasis, after severe injury is necessary to prevent major blood loss and death from hemorrhagic shock. Clots are formed initially by a platelet plug that is then reinforced by a fibrin fiber network. However, the depletion and rapid consumption of functional circulating clotting factors after large volume blood loss prevents the formation of robust fibrin networks (2, 3). Furthermore, activation of profibrinolytic pathways causes accelerated breakdown of fibrin matrices, or hyperfibrinolysis (4). The resulting clots are therefore weak and insufficient to stop bleeding. This acquired coagulopathy, known as trauma-induced coagulopathy (TIC), is observed in 25% of trauma patients (2) and is associated with increased mortality (3). Therefore, methods to augment or restore hemostatic function are needed to prevent hemorrhage-related deaths.

Although there are several well-established topical hemostatic agents used to resolve bleeding in external injuries (e.g. pressure dressings, gel sealants) (5), there are few examples of systemically administered hemostatic agents to stop bleeding in non-compressible internal injuries. Factor replacement by transfusion of blood components (i.e. fresh frozen plasma, fibrinogen concentrate) or recombinant proteins is the standard approach to restoring hemostatic function (6). However, blood components are costly, have special storage requirements and limited shelf-life, and carry risk of immunogenicity or viral transmission (7). Therefore, there is a critical unmet need for intravenously administered hemostatic agents that can reach distant inaccessible bleeding sites and bolster clot formation after traumatic injury, without the aforementioned complications.

In the past decade, several synthetic platelet platforms have been reported to induce faster blood clotting after intravenous injection. Notable examples include poly (lactic-co-glycolic acid)–poly-L-lysine–poly (ethylene glycol)–[Arg-Gly-Asp] (PLGA-PLL-PEG-RGD) nanoparticles that interact with platelet integrin GPIIb–IIIa to induce platelet aggregation (8) and peptide-modified liposomes that mimic platelet adhesion, aggregation, and activation (9–12). However, a challenge with nanoparticle-based approaches is their rapid clearance by the reticuloendothelial system (13). Furthermore, the focus on platelet substitutes leaves the clot's fibrin compartment largely ignored. A fibrin-targeted approach to hemostasis acting downstream of initial platelet plug formation may provide a safer alternative to platelet substitutes to avoid undesired thrombotic events.

Fibrin is a viscoelastic biopolymer produced at the site of vascular injury by the coagulation cascade. Locally activated thrombin enzyme cleaves circulating fibrinogen to form fibrin monomers. Fibrin monomers self-polymerize in a half-staggered, double-stranded manner to form protofibrils, which then associate non-covalently, bundle into fibers, and branch to

form a three-dimensional insoluble hydrogel scaffold for platelets, blood cells, and other clot components (14). The transglutaminase Factor XIIIa (FXIIIa) then stabilizes the clot by creating intra- and inter-fiber crosslinks through amide bond formation between lysine and glutamic acid residues. FXIIIa supplementation has been shown to produce fibrin networks with thinner fiber diameters, greater fiber density, and smaller pores for a given fibrinogen concentration than fibrin not supplemented with FXIIIa (15, 16). These architectural changes contribute to increased clot stiffness and resistance to fibrinolysis.

Drawing inspiration from FXIIIa, we engineered a synthetic hemostatic polymer, PolySTAT, that stabilizes blood clots through fibrin crosslinking. Although FXIII crosslinks fibrin via covalent bond formation, we hypothesized that similar clot-stabilizing effects could be achieved using a polymer forming multiple non-covalent bonds to adjacent fibrin monomers. Moreover, the incorporation of synthetic polymers resistant to degradation by the plasmin enzyme would inhibit fibrinolysis. When evaluated *in vitro* under coagulopathic and hyperfibrinolytic conditions, PolySTAT accelerated clotting kinetics, increased clot strength, and delayed clot breakdown. Intravenous administration of PolySTAT in rats before and after femoral artery injury reduced blood loss, improved tissue perfusion with reduced fluid resuscitation requirements, and significantly improved survival rates, thus demonstrating the hemostatic function of PolySTAT and its potential for clinical translation.

RESULTS

Design of fibrin-crosslinking hemostatic polymers

We designed a synthetic polymer to mimic FXIIIa-mediated fibrin stabilization by displaying multiple fibrin-binding domains on a linear water-soluble (hydroxyethyl)methacrylate (HEMA) and *N*-hydroxysuccinimide methacrylate (NHSMA) polymer backbone [p(HEMA-*co*-NHSMA)] (Fig. 1A). This approach allowed for fibrin crosslinking to increase clot stiffness and incorporation of synthetic polymers resistant to plasmin degradation. For safe, *in situ* fibrin crosslinking after intravenous administration, hemostatic polymers must demonstrate high specificity for fibrin to prevent nonspecific binding to soluble fibrinogen or other plasma proteins that may lead to thrombotic events, such as stroke or embolism. A cyclicfibrin-specific peptide ($K_{d, \text{human}} = 121 \text{ nM}$), developed by Kolodziej et al. (17, 18), was selected as the fibrin-binding domain owing to its high binding affinity and specificity for fibrin, cross-species reactivity, extensive characterization and sequence optimization for improved binding affinity and serum stability, and previous use in humans (Fig. 1A).

Poly(HEMA) has been used clinically in implants (19) and was copolymerized here with the NHSMA monomer via reversible addition-fragmentation chain-transfer (RAFT) to provide sites for peptide grafting. This monomer ratio was chosen to be able to graft several peptides (expected conjugation efficiency of ~50%) to the polymer backbone without experiencing solubility issues from 20% NHSMA content. The degree of polymerization (DP) was 200, with a targeted molecular weight nearing the upper end of the renal threshold after peptide conjugation to prevent rapid clearance after intravenous administration (20).

PolySTAT and non-binding scrambled control polymer, PolySCRAM, were synthesized by conjugating the fibrin-specific peptide and scrambled non-binding peptide, respectively, to p(HEMA-co-NHSMA) via the ϵ -amine in a lysine introduced at the C-terminus of the peptide. The final molecular weights of PolySTAT and PolySCRAM were 45 and 47 kDa, respectively (Fig. 1B). Peptide conjugation efficiencies were approximately 40%, resulting in 16 peptides per polymer. Multivalency enhances affinity of the polymer to fibrin owing to avidity effects (21) and, in this instance, is also expected to facilitate fibrin crosslinking. Fluorescent analogues of PolySTAT and PolySCRAM (fPolySTAT and fPolySCRAM, respectively) with 2% fluoresce in methacrylate (FMA) in the polymer backbone were synthesized for imaging and contained comparable peptide content (35–45% conjugation efficiency) (Fig. 1B).

Hemostatic polymer integration and alteration of fibrin clot structure

To confirm the selective integration of PolySTAT into fibrin fibers, fPolySTAT, fPolySCRAM, and PBS were each mixed with fluorescently labelled fibrinogen, and fibrin was formed by adding thrombin prior to confocal imaging. fPolySTAT fluorescence exhibited fiber morphology which coincided with fluorescence from fibrin fibers whereas fPolySCRAM signal showed no distinct morphology (Fig. 1C), demonstrating that incorporation of fibrin-specific peptide sequences in PolySTAT is necessary for polymer integration into fibrin networks. Furthermore, fPolySTAT fluorescence was observed throughout fibrin fibers, suggesting that PolySTAT is actively integrated during the polymerization process.

Precursory analysis of fibrin clot structure was completed using turbidity measurements to determine if PolySTAT integration induced changes in fibrin structure (Fig 2A). PolySTAT-integrated clots had significantly greater turbidities compared to control clots formed with PBS or PolySCRAM, indicating structural differences in fiber diameter, density, or homogeneity (22). Turbidities of fibrin crosslinked by human Factor XIIIa (hFXIIIa) had significantly lower turbidities compared to control clots, demonstrating that covalent crosslinking by hFXIIIa versus non-covalent crosslinking by PolySTAT result in two very different fibrin architectures.

Permeation studies and SEM imaging were used to further interrogate fibrin structure. Fluid flow through PolySTAT-integrated fibrin clots was noticeably hindered compared to fibrin formed with PBS or PolySCRAM, reflecting 1.5-fold smaller pore radii in PolySTAT clots (Fig. 2B). Interestingly, 250 $\mu\text{g}/\text{ml}$ (5 μM) PolySTAT (concentration for a minimum of 2 fibrin-binding sites per PolySTAT) created smaller pore sizes than a physiological concentration of 10 $\mu\text{g}/\text{ml}$ (63 nM) hFXIIIa. SEM imaging revealed trends in pore size consistent with the permeation study (Fig. 2C). PolySTAT-modified fibrin had smaller pores interspersed throughout a dense fibrin mesh compared to PBS and PolySCRAM controls and hFXIIIa-crosslinked fibrin, which all had distinct, loosely interwoven fibers and larger pore sizes. The denser fibrin structure of PolySTAT would likely cause greater light scattering and account for the greater turbidity observed (Fig. 2A).

Hemostatic polymer increases fibrin clot strength and reduces fibrinolysis

Mortality is dramatically increased in trauma patients when fibrinogen concentrations fall below a critical threshold of 2.29 mg/ml (23, 24). Fibrin clots were formed *in vitro* with fibrinogen concentrations below threshold, at threshold, and at the average physiological concentration above threshold (25) (1.5, 2.2, and 3.0 mg/ml fibrinogen, respectively), with and without PolySTAT (5 μ M), to determine if clot strength could be rescued through PolySTAT-induced fibrin crosslinking. For each fibrinogen concentration, storage moduli (a measure of clot elasticity) of PolySTAT-modified fibrin clots were 2- to 3-fold greater than those of controls (Fig. 3A). At 1.5 mg/ml fibrinogen, PolySTAT-induced crosslinking resulted in storage moduli comparable to those of control clots at the threshold. At 2.2 mg/ml fibrinogen, the storage modulus of PolySTAT-modified fibrin was well above the threshold and greater than storage moduli of controls formed with 3 mg/ml fibrinogen. Thus, reduced clot elasticity owing to fibrinogen depletion was reversed through PolySTAT-induced crosslinking.

Thrombelastography (TEG) is a clinical viscoelastic tool that provides quantitative values for clotting onset time, clotting rate (α -angle), maximum clot strength (maximum amplitude), and, under lysing conditions, percent of clot lysed 30 minutes after time to maximum clot strength (Ly 30%). Polymers were tested by TEG in an *in vitro* hyperfibrinolytic system to determine the effects of PolySTAT on clots under the coagulopathic conditions observed in patients after the early stages of severe hemorrhage (Fig. 3, B to E, 1.5 mg/ml fibrinogen). In clotting solutions with low fibrinogen concentration, PolySTAT accelerated clot strengthening (earlier clotting onset times and ~20% faster clotting rates), produced a 2-fold increase in clot strength, and reduced Ly30% by 15% compared to PBS and PolySCRAM controls. When fibrinogen concentration was doubled, clot strength of PolySTAT-integrated clots was 1.5-fold greater than controls, and Ly30% was reduced by 39–57%. Increased clot strength combined with reduced lysis consistently resulted in clots with longer lifetimes.

hFXIIIa was supplemented at three different concentrations previously shown to increase clot strength and inhibit fibrinolysis (15, 16) for comparison to PolySTAT activity. hFXIIIa was more effective when there was a greater availability of fibrin (Fig. 3, B–E). At 3 mg/ml fibrinogen, a trend of increasing clot strength was observed with increasing hFXIIIa concentration whereas no increased clot strength was observed at 1.5 mg/ml fibrinogen (Fig. 3C). Additionally, at the higher fibrinogen concentration hFXIIIa significantly reduced clotting onset time and Ly30% (Fig. 3, B and E). PolySTAT reduced lysis to the same extent as 30 μ g/ml hFXIIIa and 20 μ g/ml hFXIIIa at 1.5 and 3 mg/ml fibrinogen, respectively (Fig. 3E). In additional TEG studies, PolySTAT-treated clots consistently showed improvement of clot formation and extended clot lifetime over a range of biologically relevant fibrinogen and plasmin concentrations (fig. S1). These effects were only induced when the fibrin-binding peptides were conjugated to the HEMA polymer backbone (fig. S2). Equivalent concentrations of free peptide, HEMA polymer, and peptide-polymer mixtures did not produce any changes in clot formation.

PolySTAT was further evaluated in diluted whole blood used to mimic dilution effects of fluid resuscitation used to treat hypovolemia after massive blood loss (27). PolySTAT-modified blood clots experienced significantly less lysis than controls (fig. S3), suggesting that the PolySTAT would retain its clot-enhancing effects during fluid resuscitation.

Fibrinolysis was next visualized by time-lapsed confocal imaging of polymer-treated fluorescent fibrin clots exposed to plasmin *in vitro*. Images of clots taken at the leading edge at 1-minute intervals are shown in Fig. 3F. PolySTAT-integrated fibrin and hFXIII-crosslinked fibrin degraded 3-fold and 8-fold slower than PBS and PolySCRAM controls (Fig. 3F, movies S1 to S4).

Hemostatic efficacy of PolySTAT in a rat femoral artery injury and fluid resuscitation model

Mechanical strengthening of clots is necessary for more effective fluid resuscitation without further blood loss induced by increasing blood pressure. To evaluate the effect of PolySTAT on clot formation *in vivo*, PolySTAT and controls were administered in a rat model of femoral artery injury and fluid resuscitation (Fig. 4A). In this model, polymer solution was injected intravenously in rats immediately following the onset of bleeding from a 3-mm incision in the femoral artery. During the first 15 min, the wound was allowed to bleed or clot without interference (free bleeding). After 15 min, saline was infused at a fixed rate of 3 ml/kg/min, when needed, to recover and maintain BP above 60 mmHg (fluid resuscitation). Blood loss was tracked by collecting blood with pre-weighed gauze. Hemorrhage volumes during fluid resuscitation are indicative of the stability of clots formed during free bleeding. Weaker clots are more susceptible to rebleeding as blood pressure increases and would result in greater blood loss.

Dilutional coagulopathy after fluid resuscitation was confirmed in this model by tracking prothrombin time (PT), plasma fibrinogen concentration, hemorrhage volumes, blood pressure, and blood lactate concentrations in rats injected with a volume control (0.9% saline) to account for effects of bolus fluid administration on bleeding. Prolonged PT, indicating longer clotting time, is a hallmark of trauma-induced coagulopathy (TIC) in humans and animal models, and rat models of TIC experience precipitous falls in fibrinogen concentration and elevated lactate levels after trauma (28). Lactate, a byproduct of anaerobic respiration, is released into circulation owing to inadequate tissue perfusion and indicates the presence and severity of hemorrhagic shock. Lactate concentration and clearance from the blood are established predictive markers for trauma patient mortality (29) and were measured to determine the efficacy of fluid resuscitation. In our model, blood loss from the catheter hemorrhage and free bleeding phase resulted in shortening of PT, a 1.8-fold drop in fibrinogen concentration, and increased lactate levels. All rats required fluid resuscitation after free bleeding. Despite fluid infusion, animals remained hypo-perfused. BPs remained below 60 mmHg and lactate levels continued increasing to 30 min. Saline infusion resulted in prolonged PT compared to baseline values.

Following characterization of the TIC model, rats were injected with PolySTAT, PolySCRAM, rat albumin, or hFXIIIa immediately after bleeding (t=0 min). Polymers and rat albumin were injected at 15 mg/kg, a dose replicating concentrations used *in vitro*. Rat

albumin was used to control for changes in intravascular oncotic pressures owing to polymer size. For comparison of *in vivo* efficacy, hFXIIIa was administered at 1.92 mg/kg for an initial circulating concentration of 30 µg/ml, a concentration shown to have comparable or greater lysis-reducing effects as 15 mg/kg PolySTAT in TEG studies. Vital measurements (prothrombin time, fibrinogen, blood pressure, and lactate) for each animal are provided in fig. S4–S7. All animals (100%, $n = 5$) treated with PolySTAT following injury survived to the end of protocol whereas 0–40% of animals injected with the volume control, PolySCRAM, albumin, and hFXIIIa survived (Fig. 4B). Of the animals surviving the full protocol time (9 of 25), none experienced rebleeding during fluid resuscitation, meaning that clots formed during the free bleeding period were strong enough to withstand increasing blood pressure from saline infusion (Fig. 4C).

All PolySTAT-treated animals survived, indicating that PolySTAT is able to assist in forming stronger clots more resistant to rupture. Owing to no incidences of rebleeding (Fig. 4C), PolySTAT-treated animals experienced up to 11-fold less blood loss than controls (Fig. 4D) and five foldless saline was needed to maintain BP at 60 mm Hg compared with all other treatment groups (Fig. 4E). Although volume controls used $97 \pm 6\%$ of the maximum allowed infusion volume, PolySTAT-treated animals required only $42 \pm 17\%$ of the maximum allowed infusion volume to maintain a BP of 60 mmHg. Lower fluid resuscitation volumes can be attributed to robust clot formation, which prevents the loss of infused volumes from the wound.

Owing to the number of early deaths in PolySCRAM, albumin, and hFXIIIa treatment groups, statistical comparison was completed between PolySTAT and volume controls for comparison of BP and lactate levels. PolySTAT-treated rats had significantly higher blood pressures (mean arterial pressure, MAP) (Fig. 4F, fig S6) and lower lactate levels (Fig. S7) compared to volume controls, indicating that tissues were better perfused in PolySTAT-treated animals.

Biodistribution of hemostatic polymers

The pharmacokinetics and biodistribution of PolySTAT was determined in healthy rats (Fig. 5). Radio labeled PolySTAT was administered intravenously at the equivalent dose used in femoral artery injury studies (15 mg/kg). Blood was collected at various time points after injection followed by perfusion and organ collection. The initial distribution half-life of PolySTAT was 20 min ($t_{1/2,\alpha}$) and the elimination half-life was 14.4 hr ($t_{1/2,\beta}$) (table S2). Elimination half-life and distribution rate from the central compartment to peripheral compartment (k_{12} , 0.0238 min^{-1}) are similar to reported values for 50-kDa polyethylene glycol (PEG) ($t_{1/2,\beta}$ of PEG50k = 16.5 h; $k_{12} = 0.02 \text{ min}^{-1}$). PEGylation is a technique used to increase circulation times in several FDA-approved biologic drugs.

The majority of PolySTAT (>50%) was cleared from the body within 1 h. The remaining polymer was distributed primarily to the liver (~16% of initial injected dose, I.D.) and kidney (21% of I.D.) (Fig.5A). The amount of PolySTAT accumulation in liver and kidney increased after injection to 1 h but then started to decrease by 24 h, indicating elimination from the body. The slower elimination from kidneys and liver is likely due to low transfer rate from the tissues back into blood ($k_{21} \sim 0.003/\text{min}$; 5.5-fold lower than PEG50k) (30).

Normalization of total PolySTAT content to organ mass demonstrated PolySTAT concentrations in the spleen similar to those in the liver (Fig. 5B). No PolySTAT accumulated in the heart and lungs at any time. PolySTAT was primarily removed from circulation by renal clearance. Tritium counts for urine collected within the first 30 minutes after injection confirmed elimination by renal filtration (table S3).

Metabolic and hepatic function panels were completed at 1 h, 1 day, and 1 week after PolySTAT injection to assess liver and kidney function (table S1). Creatinine levels, used to indicate kidney function, were slightly elevated 1 hour after polymer injection, which is likely due to the monopolization of glomerular filtration by significantly larger PolySTAT. By 1 day after injection, creatinine levels returned to control levels indicating that any effect of the polymer on renal filtration is reversible. Indicators of hepatic function, such as plasma concentrations of albumin and bilirubin, showed no significant changes compared to rats receiving no injection. Liver-associated enzymes alkaline phosphatase and alanine amino transferase (ALT) also showed no significant changes in concentration compared to rats receiving no injection. Rats showed no signs of distress post-injection and had healthy weight gain until time of euthanasia. Thus, PolySTAT treatment at clinically relevant doses was well-tolerated in rats.

Discussion

The goal of this work was to develop a synthetic hemostatic polymer (PolySTAT) that, when administered systemically, would accumulate locally at sites of vascular injury and induce hemostasis. Fibrin-crosslinking occurs naturally *in vivo* by FXIIIa-catalyzed peptide bond formation between glutamic acid and lysine residues. Although these crosslinks are covalent in nature, we hypothesized that a synthetic polymer binding non-covalently to adjacent fibrin monomers could recapitulate similar clot-strengthening effects as well as prevent enzymatic breakdown through introduction of plasmin-resistant polymers into fibrin fibers. PolySTAT was synthesized by grafting fibrin-binding peptides onto a linear polymer backbone synthesized by living polymerization. Fibrin fibers contain anywhere from tens to hundreds of double-stranded protofibrils each with up to 25 half-staggered fibrin monomers (31). Therefore, peptide-binding sites are in abundance for PolySTAT activity.

The fibrin-binding peptide used here was previously identified using phage display and was found to have two binding sites per fibrin monomer, which is attributed to the dimeric structure of fibrin (17, 18). Although the binding sites are still unknown, this peptide does not induce fibrinogen self-association and does not inhibit fibrin formation and thus minimizes the possibility of thrombosis or exacerbated bleeding after intravenous injection. Binding of this peptide to fibrin is conserved across multiple species, including humans, pigs, and rats (32), and is therefore opportune for both preclinical development and clinical translation. This peptide has also been shown to selectively accumulate in fibrin-rich thrombi and was well-tolerated when administered intravenously in humans (33). Given its specificity for fibrin and the extensive optimization and characterization, this fibrin-binding peptide was the ideal targeting ligand for PolySTAT construction.

When mixed into clotting solutions, PolySTAT self-integrated into fibrin fibers and produced dense fibrin meshes with smaller pores. Although this architecture is vastly different from FXIIIa-crosslinked fibrin, similar clot-stabilizing effects were achieved in regard to inhibiting fibrinolysis. TEG studies in which plasmin is present throughout the initial clotting solution suggest the slower rate of fibrinolysis in PolySTAT-integrated fibrin is due to the resistance of the altered fibrin itself to enzymatic breakdown rather than a sole function of limited plasmin diffusion. Inhibition of fibrinolysis allowed PolySTAT-modified fibrin to maintain greater clot strength than PBS and PolySCRAM controls over longer periods of time which is desirable for preventing rebleeding. Furthermore, the ability of PolySTAT to restore clot strength to fibrin formed at fibrinogen concentrations below the critical threshold suggests that PolySTAT can be an alternative to fibrinogen concentrates which are currently used in European trauma centers (26). When administered intravenously, PolySTAT improved survival by reducing blood loss and preventing rebleeding during fluid resuscitation in injured rats, thereby maintaining higher BP and minimizing the need for saline infusion. Reduced fluid resuscitation requirements are beneficial as fluid resuscitation is known to exacerbate bleeding due to increased blood pressures as well as dilution of circulating clotting factors (34).

Prior to this work, efforts to develop intravenous hemostats were predominantly focused on synthetic platelet substitutes. Nanoparticles functionalized with peptide ligands for binding subendothelial matrix proteins and surface glycoproteins on platelets have been used to mimic platelet adhesion and aggregation (8–12). Initial platelet plug formation is important for blood clotting. However, as shown here, mechanical and degradative properties of the clot's fibrin compartment can be tuned using synthetic polymers to prolong clot lifetime and, thus, presents an alternative strategy for inducing hemostasis. Because PolySTAT's mechanism of action targets a different step in the clotting process from synthetic platelets, there are opportunities for these technologies to work synergistically.

In addition, although nanoparticles have been reported to be rapidly sequestered by the reticuloendothelial system (RES) (35), water-soluble polymers show molecular weight-dependent circulation half-lives and reduced RES accumulation compared to nanoparticles (30). As much as 70% of injected doses of systemically administered nanoparticle hemostats accumulate in the liver within the first 10 minutes of circulation and is retained for up to 1 day (8), whereas liver accumulation of PolySTAT was not detected above 23% of the injected dose. Thus, relative to particle systems, higher PolySTAT concentrations are maintained circulating in the blood at earlier timepoints. Longer circulation times combined with rapid activity during fibrin polymerization is advantageous for resolving bleeding during transport of trauma patients to a Level 1 trauma center, which is generally within the hour after injury (36). Pharmacokinetic studies revealed that 7% of PolySTAT remains in kidneys one week after administration, which is likely accumulation of polymer from the larger end of the molecular weight distribution. Future generations of PolySTAT may be synthesized at lower DP to ensure more complete renal clearance.

One of the largest concerns when administering intravenous hemostats is off-target clot formation leading to thrombotic events such as stroke or heart attack. Binding specificity of PolySTAT to fibrin minimizes risk of thrombosis by ensuring that PolySTAT does not bind

and crosslink the circulating fibrin precursor (fibrinogen). Thus, the clot is localized at the site of injury. Furthermore, the eventual elimination from circulation as we see with PolySTAT is favorable for preventing thrombosis. PolySTAT-crosslinked clots are expected to be removed during surgical repair of the injury once the patient has been transported to the hospital. However, should PolySTAT-integrated clots remain in the body, fibrinolysis is simply delayed, not completely eliminated.

For trauma patients surviving the initial 24 hours after injury, the greatest concerns are renal injury, lung injury, and multiple organ failure (37). Therefore, further evaluation is needed to determine if PolySTAT treatment will reduce the extent of organ injury in surviving animals. In addition, pharmacokinetics and evaluation of hemostatic effects in larger animal models such as pig models are necessary before clinical translation.

Acute bleeding caused by traumatic injury requires quick resolution to prevent exsanguination, and PolySTAT shows great promise as a fast-acting systemic hemostat to enhance clotting in bleeding patients. However, the hemostatic mechanism of PolySTAT is dependent on fibrin formation. If thrombin activation or activity is inhibited owing to severe depletion of coagulation factors or use of anticoagulant drugs (e.g. warfarin), fibrin will be unavailable for PolySTAT crosslinking. In this case, co-administration of blood products may be the fastest way to restore fibrin formation for PolySTAT crosslinking. Another instance in which PolySTAT efficacy may be reduced is in the presence of high concentrations of fibrin degradation products. Depending on the PolySTAT-fibrin binding site, it is possible that circulating D-dimers in hyperfibrinolytic patients may compete with clots for PolySTAT binding, thus reducing efficacy.

Collectively, we have demonstrated that polymers can be engineered to recover or augment natural processes in clot formation to treat acute bleeding. More specifically, preparation of polymers by RAFT polymerization enables reproducible and scalable material synthesis and, thus, offers production, storage, and safety advantages over current biologic-based treatments for bleeding. Furthermore, polymers are versatile drug delivery platforms and can be engineered to include other (macro) molecules, such as antifibrinolytic drugs or inhibitors of anticoagulant proteins, for added functionality. Although PolySTAT was evaluated in this work for inducing hemostasis in acquired coagulopathy, it can also potentially be used to treat acute bleeding episodes in congenital clotting disorders such as FXIII deficiency and used in combination with recombinant clotting factor therapies for hemophilia.

Materials and Methods

Study design

Hemostatic polymers were administered intravenously in a rat femoral artery injury model to determine hemostatic efficacy *in vivo*. The protocol was approved by the University of Washington Institutional Animal Care and Use Committee (IACUC). For a power of 0.8 and significance value of 0.05, 5 rats were needed per treatment group. The treatment groups include rats intravenously injected with a volume control (0.9% saline), PolySTAT, PolySCRAM, hFXIIIa, and rat albumin. Rat albumin, which has comparable molecular weight to PolySTAT and PolySCRAM, was used as a control for changes in oncotic

pressure due to polymer circulation. The following measurements were taken before and after injury to monitor the condition of the rat and performance of the polymers: blood pressure collected continuously via a transducer connected to a catheter and BIOPAC unit, lactic acid concentration in sampled blood using a radiometer, blood loss by collection with pre-weighed gauze, and saline infusion volumes recorded from the syringe pump. Surgical procedures, control/polymer injection, radiometer measurements, blood collection, and saline infusion were completed by a researcher blinded to the treatment. Blinding was ensured by a second researcher who prepared controls and hemostatic polymer solutions in randomized order. Measurements were recited by the blinded researcher to the second researcher who would record values under a numerical-alphabetical identification number assigned to each rat. Rats with high baseline lactic acid concentrations (> 1.0 mM) and rats experiencing apnea that could not be revived by chest compressions before the 10 min time point were excluded from studies. The endpoint of studies was reached when blood pressure dropped below 20 mmHg, at which point rats were euthanized with an overdose of pentobarbital. Data were compiled and sent to a third researcher for statistical analysis.

Synthesis and characterization of hemostatic polymers (PolySTAT) and scrambled polymer controls (PolySCRAM)

All materials for poly(HEMA) backbone (pHB) synthesis were purchased from Sigma-Aldrich. pHB with a target composition of 80% (hydroxyethyl) methacrylate (HEMA) and 20% *N*-hydroxysuccinimide methacrylate (NHSMA) was synthesized using RAFT polymerization. For a typical synthesis, 310 μ L HEMA (2.56 mmol), 117.2 mg NHSMA (0.640 mmol), 1 mL 2,2'-azobis(isobutyronitrile) (AIBN) (0.876 mg/ml in dimethylacetamide, 0.0053 mmol), and 4.47 mg 4-cyanopentanoic acid dithiobenzoate (CPADB) (0.016 mmol) were dissolved in a 5-mL reaction vessel with 3.02 mL dimethylacetamide (DMAc) for a final monomer concentration of 0.6 M. The reaction mixture was purged with argon for 10 minutes and reacted under stirring conditions at 70°C for 24 hr. Fluorescent hemostatic polymer (fPolySTAT) and scrambled polymer control (fPolySCRAM) were synthesized by altering the composition of pHB to 78% HEMA and 2% fluorescein *O*-methacrylate and maintaining 20% NHSMA. Polymers were precipitated in ether, dissolved in DMAc, and reprecipitated in ether to remove unreacted monomers. Polymers were then dried and stored in a vacuum-sealed oven. Dithiobenzoate groups were removed in a subsequent reaction with a 20:1 molar ratio of AIBN to polymer. Transition of the solution from pink to clear was a positive indicator that the endcapping reaction was near or at completion. Degree of polymerization and monomer composition were determined using H^1 NMR, and polydispersity and molecular weight were measured using GPC. The absence of CTA peaks on H^1 NMR was used to confirm removal of dithiobenzoate groups. Fibrin-binding peptides with the sequence Ac-Y(DGI)C(HPr)YGLCYIQGK and a scrambled peptide sequence Ac-YICGQ(DGI)AC(HPr)LYGK with the same modifications were purchased from GL Biochem at >95% purity. Fibrin-binding peptides were conjugated to NHS reactive groups on pHB via the ϵ -amine on the C-terminus lysine under organic basic reaction conditions as reported by Yanjarappa et al. (38). Scrambled peptides were conjugated to NHS groups on pHB for the scrambled polymer control. After 24 h, reaction solutions were transferred to snakeskin dialysis tubing with 10kDa MWCO and dialyzed against PBS for 2 days to remove free peptide. Polymers were then dialyzed against DI

water for 2 days to remove salts from the PBS and lyophilized. The number of peptides per polymer was determined by measuring absorption at 280 nm using a Nanodrop 2000 UV-vis spectrophotometer.

Confocal imaging of pure fibrin clots to show co-localization of hemostatic polymers and fibrin

Fibrin clots were prepared in chambered coverslips using 0.5 mL clotting solution with the following final concentrations: 3 mg/ml fibrinogen spiked with 1% Alexa Fluor 546-labeled fibrinogen (Life Technologies F13192), 0.167 IU/mL thrombin, 10 μ M CaCl₂, and 5 μ M fluorescent PolySTAT, 5 μ M fluorescent PolySCRAM, or an equal volume of PBS. After 1 hr, clots were imaged with a Zeiss LSM 510 inverted confocal microscope using a 63 \times objective lens. Lasers with 488 nm and 543 nm wavelength were used to excite polymers and fibrinogen, respectively. BP 505–530 and LP 560 were used to isolate signal from polymers and fibrinogen, respectively. To prevent bleed-through, only one laser was turned on at a time during image acquisition. Image overlays were completed in Image J.

***In vitro* evaluation of PolySTATs using thromboelastography**

In a typical TEG experiment, a 360- μ L clotting solution is added to a cup in a TEG 5000 Thromboelastograph Hemostasis Analyzer system. A pin attached to a torsion wire is submerged into the center of the cup. When the device is started, the cup oscillates around the stationary pin and as the clot forms, the movement of the pin becomes coupled with the cup. The amplitude of oscillatory motion of the pin, which is directly proportional to clot strength, is measured over time. Other measures that can be extracted from TEG traces include clot onset time (R), clotting rate (α -angle in degrees), maximum clot strength (maximal amplitude in mm, MA), and the extent of lysis 30 minutes after the time to MA (ly30%). PolySTAT, PolySCRAM, pHB stock solutions were made at 250 μ M and free peptide stock solution at 4 mM. 7.2 μ L volumes were added to clotting solutions for final concentrations of 5 μ M and equivalent peptide concentration. For purified fibrin systems, the clotting solution had final concentrations of 1.5 mg/ml plasminogen-depleted fibrinogen, 0.5 IU/mL thrombin (StagoFibriPrest Automate 5), 2 μ g/ml plasmin (Enzyme Research Laboratories), and 10 mM CaCl₂ in pH 7.4 NaCl-HEPES buffer (44 mM HEPES, 2 mM CaCl₂, 140 mM NaCl). Fibrinogen was added to the enzymes and CaCl₂ immediately before each TEG run. For evaluation in hemodilutions, citrated fresh human blood was diluted at 1:1, 1:2, and 1:3 parts blood to 0.9% saline. 333 μ L of Hemodilutions was mixed with 20 μ L 0.2M CaCl₂ solution and 7.2 μ L volumes of PolySTAT or controls.

Hemostasis in a rat femoral artery injury and fluid resuscitation model

Sprague Dawley rats weighing 310–360g were randomized into one of five treatment groups (volume control, PolySTAT, PolySCRAM, rat albumin, or human Factor XIIIa). Rats were anesthetized using isoflurane and 0.1 mL ketamine-xylazine cocktail (87.5 mg/ml ketamine, 12.5 mg/ml xylazine) injection in the hindlimb. The carotid artery and jugular vein were catheterized for monitoring of blood pressure and for intravenous injection of polymers, respectively. Blood gas and metabolite measurements were completed to confirm that baseline respiration and lactate levels were within acceptable ranges (carbon dioxide, < 55mmHg; O₂ saturation, > 95%; lactate, <1.0 mM).

Once normal respiration and lactate levels were established, the femoral artery in the left leg was isolated and microsurgical clamps were placed proximally and distally to prevent bleeding from a 3-mm longitudinal incision made after clamping. Controlled catheter bleeds were then completed via the arterial line to normalize all starting blood pressures to 40–50 mmHg. Immediately following catheter bleeds, clamps were removed from the femoral artery ($t = 0$ min), and the wound was allowed to bleed freely or clot without interference for 15 min. Immediately after clamp release, PolySTAT, PolySCRAM, or rat albumin in a 10 mg/ml solution was administered over 1.5 minutes at a dose of 15 mg/kg. hFXIIIa was administered at 1.92 mg/ml for an initial circulating concentration of 30 μ g/ml, a dose shown to have crosslinking effects in vitro in TEG studies. For $t > 15$ min, fluid resuscitation in the form of saline infusion at 3 mL/min/kg was used to restore and maintain BP above 60 mmHg. Infusion volumes were capped at 60 mL/kg.

Arterial lines for blood pressure monitoring were flushed when waveforms were dampened from clot formation in the line which occurred sporadically when blood pressure was low. Blood gas measurements were taken before femoral artery injury (baseline), right after the free bleeding phase ($t = 15$ min), during the fluid resuscitation phase ($t = 30$), and at the protocol endpoint if the animal survived ($t = 75$ min) to monitor blood pH, gas levels, ion concentrations, and lactate concentration. Blood adjacent to the wound was collected by the blinded researcher using pre-weighed gauze to track blood loss over time. Care was taken to not touch or otherwise disturb the vessel or the forming clot.

Biodistribution studies

Radiolabeled PolySTAT was synthesized by mixing in tritiated glycine (Perkin Elmer) to fibrin-binding peptides for conjugation to p(HEMA-co-NHSMA) copolymers (1 glycine for every 200 PolySTAT). Rats were anesthetized using isoflurane and ketamine-xylazine cocktail injection in the hindlimb. 15 mg/kg radiolabeled PolySTAT was administered via tail-vein injection. At the desired timepoints (5 min, 10 min, 20 min, 1 hr, and 1 day), the thoracic cavity was opened and blood was collected from the right atrium of the heart using a syringe. Rats were then perfused, and organs were rinsed, weighed, and homogenized. Tissue homogenates were solubilized using Solvable (Perkin Elmer) for 2 hours at 50°C and decolorized for 4–6 hours by addition of 30% (v/v) hydrogen peroxide and 100 mM EDTA solution to prevent bubbling. 20 μ L 10 N HCl and 10 mL Ultima Gold (Perkin Elmer) was then added and samples were shaken vigorously and allowed to sit overnight before reading in a scintillation counter.

Statistical analysis

One-way ANOVAs with TukeyKramer post hoc tests were completed on data from TEG studies and animal studies (hemorrhage volume, saline infusion rate) using GraphPad Prism 5 and JMP statistical software to determine significance and calculate p-values. Differences between groups were considered statistically significant when $p < 0.05$. Two-way ANOVAs were completed for comparison of MAP and lactate concentrations between volume controls and animals receiving PolySTAT. A log-rank Mantel-Cox test was completed to determine significance of survival data for in vivo studies.

Supplementary Material

Refer to Web version on PubMed Central for supplementary material.

Acknowledgments

We thank E.B. Lim and R.J. Lamm for assistance with animal studies, J.C. Phan and C.S. Ball for their technical expertise with SEM imaging, and P.D. Iglesia for his technical expertise in rheometry.

Funding: Supported by NIH 1R21EB018637, the Institute of Translational Health Sciences (ITHS), the Washington Research Foundation (SHP), grant KL2 TR000421 from the NIH National Center for Advancing Translational Sciences (NJW), and the Bioengineering Cardiovascular Training Grant NIH 2T32EB001650-06A2 (LWC).

References and Notes

1. Sauaia A, Moore FA, Moore EE, Moser KS, Brennan R, Read RA, Pons PT. Epidemiology of trauma deaths: a reassessment. *J Trauma*. 1995; 38:185–193. [PubMed: 7869433]
2. Davenport R, Manson J, De'Ath H, Platton S, Coates A, Allard S, Hart D, Pearse R, Pasi KJ, MacCallum P, Stanworth S, Brohi K. Functional definition and characterization of acute traumatic coagulopathy. *Crit Care Med*. 39:2652–2658. [PubMed: 21765358]
3. Brohi K, Singh J, Heron M, Coats T. Acute traumatic coagulopathy. *J Trauma*. 2003; 54:1127–1130. [PubMed: 12813333]
4. Raza I, Davenport R, Rourke C, Platton S, Manson J, Spoor C, Khan S, De'Ath HD, Allard S, Hart DP, Pasi KJ, Hunt BJ, Stanworth S, MacCallum PK, Brohi K. The incidence and magnitude of fibrinolytic activation in trauma patients. *J Thromb Haemost*. 2013; 11:307–314. [PubMed: 23176206]
5. Achneck HE, Sileshi B, Jamiolkowski RM, Albala DM, Shapiro ML, Lawson JH. A comprehensive review of topical hemostatic agents: efficacy and recommendations for use. *Ann Surg*. 2010; 251:217–228. [PubMed: 20010084]
6. Hunt BJ. Bleeding and coagulopathies in critical care. *N Engl J Med*. 2014; 370:847–859. [PubMed: 24571757]
7. Moore FA, Moore EE, Sauaia A. Blood transfusion. An independent risk factor for postinjury multiple organ failure. *Arch Surg*. 1997; 132:620–625. [PubMed: 9197854]
8. Bertram JP, Williams CA, Robinson R, Segal SS, Flynn NT, Lavik EB. Intravenous hemostat: nanotechnology to halt bleeding. *Sci Transl Med*. 2009; 1:11ra22.
9. Nishiyama T, Murata M, Handa M, Ikeda Y. Targeting of liposomes carrying recombinant fragments of platelet membrane glycoprotein Iba α to immobilized von Willebrand factor under flow conditions. *Biochem Biophys Res Commun*. 2000; 270:755–760. [PubMed: 10772897]
10. Modery CL, Ravikumar M, Wong TL, Dzuricky MJ, Durongkaveroj N, Sen Gupta A. Heteromultivalent liposomal nanoconstructs for enhanced targeting and shear-stable binding to active platelets for site-selective vascular drug delivery. *Biomaterials*. 2011; 32:9504–9514. [PubMed: 21906806]
11. Ravikumar M, Modery CL, Wong TL, Dzuricky M, Sen Gupta APD. Mimicking Adhesive Functionalities of Blood Platelets using Ligand-Decorated Liposomes. *Bioconjug Chem*. 2012; 23:1266–1275. [PubMed: 22607514]
12. Okamura Y, Takeoka S, Eto K, Maekawa I, Fujie T, Maruyama H, Ikeda Y, Handa M. Development of fibrinogen gamma-chain peptide-coated, adenosine diphosphate-encapsulated liposomes as a synthetic platelet substitute. *J Thromb Haemost*. 2009; 7:470–477. [PubMed: 19143920]
13. Jones SW, Roberts RA, Robbins GR, Perry JL, Kai MP, Chen K, Bo T, Napier ME, Ting JP, Desimone JM, Bear JE. Nanoparticle clearance is governed by Th1/Th2 immunity and strain background. *J Clin Invest*. 2013; 123:3061–3073. [PubMed: 23778144]
14. Chernysh IN, Nagaswami C, Purohit PK, Weisel JW. Fibrin clots are equilibrium polymers that can be remodeled without proteolytic digestion. *Sci Rep*. 2012; 2:879. [PubMed: 23170200]

15. Theusinger OM, Baulig W, Asmis LM, Seifert B, Spahn DR. In vitro factor XIII supplementation increases clot firmness in Rotation Thromboelastometry (ROTEM). *Thromb Haemost.* 2010; 104:385–391. [PubMed: 20431856]
16. Hethershaw EL, Cilia La Corte AL, Duval C, Ali M, Grant PJ, Ariens RA, Philippou H. The effect of blood coagulation factor XIII on fibrin clot structure and fibrinolysis. *J Thromb Haemost.* 2014; 12:197–205. [PubMed: 24261582]
17. Kolodziej AF, Nair SA, Graham P, McMurry TJ, Ladner RC, Wescott C, Sexton DJ, Caravan P. Fibrin specific peptides derived by phage display: characterization of peptides and conjugates for imaging. *Bioconjug Chem.* 2012; 23:548–556. [PubMed: 22263840]
18. Kolodziej AF, Zhang Z, Overoye-Chan K, Jacques V, Caravan P. Peptide optimization and conjugation strategies in the development of molecularly targeted magnetic resonance imaging contrast agents. *Methods Mol Biol.* 2014; 1088:185–211. [PubMed: 24146405]
19. Barrett GD, Constable IJ, Stewart AD. Clinical results of hydrogel lens implantation. *J Cataract Refract Surg.* 1986; 12:623–631. [PubMed: 3783468]
20. Duncan R. The dawning era of polymer therapeutics. *Nat Rev Drug Discov.* 2003; 2:347–360. [PubMed: 12750738]
21. Mammen M, Choi S-K, Whitesides GM. Polyvalent Interactions in Biological Systems: Implications for Design and Use of Multivalent Ligands and Inhibitors. *Angew. Chemie.* 1998; 37
22. Carr ME Jr, Hermans J. Size and density of fibrin fibers from turbidity. *Macromolecules.* 1978; 11:46–50. [PubMed: 621951]
23. Hagemo JS, Jorgensen JJ, Ostrowski SR, Holtan A, Gundersen Y, Johansson PI, Naess PA, Gaarder C. Changes in fibrinogen availability and utilization in an animal model of traumatic coagulopathy. *Scand J Trauma Resusc Emerg Med.* 21:56. [PubMed: 23867061]
24. Fries D, Martini WZ. Role of fibrinogen in trauma-induced coagulopathy. *Br J Anaesth.* 2010; 105:116–121. [PubMed: 20627882]
25. Grannis GF. Plasma fibrinogen: determination, normal values, physiopathologic shifts, and fluctuations. *Clin Chem.* 1970; 16:486–494. [PubMed: 5427531]
26. Schöchl H, Schlimp CJ. Trauma bleeding management: the concept of goal-directed primary care. *Anesth. Analg.* 2014; 119:1064–1073. [PubMed: 23757468]
27. Finfer S, Bellomo R, Boyce N, French J, Myburgh J, Norton R. A comparison of albumin and saline for fluid resuscitation in the intensive care unit. *N Engl J Med.* 2004; 350:2247–2256. [PubMed: 15163774]
28. Darlington DN, Craig T, Gonzales MD, Schwacha MG, Cap AP, Dubick MA. Acute coagulopathy of trauma in the rat. *Shock.* 2013; 39:440–446. [PubMed: 23481505]
29. Odom SR, Howell MD, Silva GS, Nielsen VM, Gupta A, Shapiro NI, Talmor D. Lactate clearance as a predictor of mortality in trauma patients. *J Trauma Acute Care Surg.* 2013; 74:999–1004. [PubMed: 23511137]
30. Yamaoka T, Tabata Y, Ikada Y. Distribution and tissue uptake of poly(ethylene glycol) with different molecular weights after intravenous administration to mice. *J Pharm Sci.* 1994; 83:601–606. [PubMed: 8046623]
31. Weisel JW, Litvinov RI. Mechanisms of fibrin polymerization and clinical implications. *Blood.* 2013; 121:1712–1719. [PubMed: 23305734]
32. Overoye-Chan K, Koerner S, Looby RJ, Kolodziej AF, Zech SG, Deng Q, Chasse JM, McMurry TJ, Caravan P. EP-2104R: a fibrin-specific gadolinium-Based MRI contrast agent for detection of thrombus. *J Am Chem Soc.* 2008; 130:6025–6039. [PubMed: 18393503]
33. Vymazal J, Spuentrup E, Cardenas-Molina G, Wiethoff AJ, Hartmann MG, Caravan P, Parsons EC Jr. Thrombus imaging with fibrin-specific gadolinium-based MR contrast agent EP-2104R: results of a phase II clinical study of feasibility. *Invest Radiol.* 2009; 44:697–704. [PubMed: 19809344]
34. Schreiber MA. Coagulopathy in the trauma patient. *Curr Opin Crit Care.* 2005; 11:590–597. [PubMed: 16292065]
35. Dobrovolskaia MA, Aggarwal P, Hall JB, McNeil SE. Preclinical studies to understand nanoparticle interaction with the immune system and its potential effects on nanoparticle biodistribution. *Mol Pharm.* 2008; 5:487–495. [PubMed: 18510338]

36. Swaroop M, Straus DC, Agubuzu O, Esposito TJ, Schermer CR, Crandall ML. Pre-hospital transport times and survival for Hypotensive patients with penetrating thoracic trauma. *J Emerg Trauma Shock*. 2013; 6:16–20. [PubMed: 23494152]
37. Brohi K, Cohen MJ, Davenport RA. Acute coagulopathy of trauma: mechanism, identification and effect. *Curr Opin Crit Care*. 2007; 13:680–685. [PubMed: 17975390]
38. Yanjarappa MJ, Gujraty KV, Joshi A, Saraph A, Kane RS. Synthesis of copolymers containing an active ester of methacrylic acid by RAFT: controlled molecular weight scaffolds for biofunctionalization. *Biomacromolecules*. 2006; 7:1665–1670. [PubMed: 16677052]

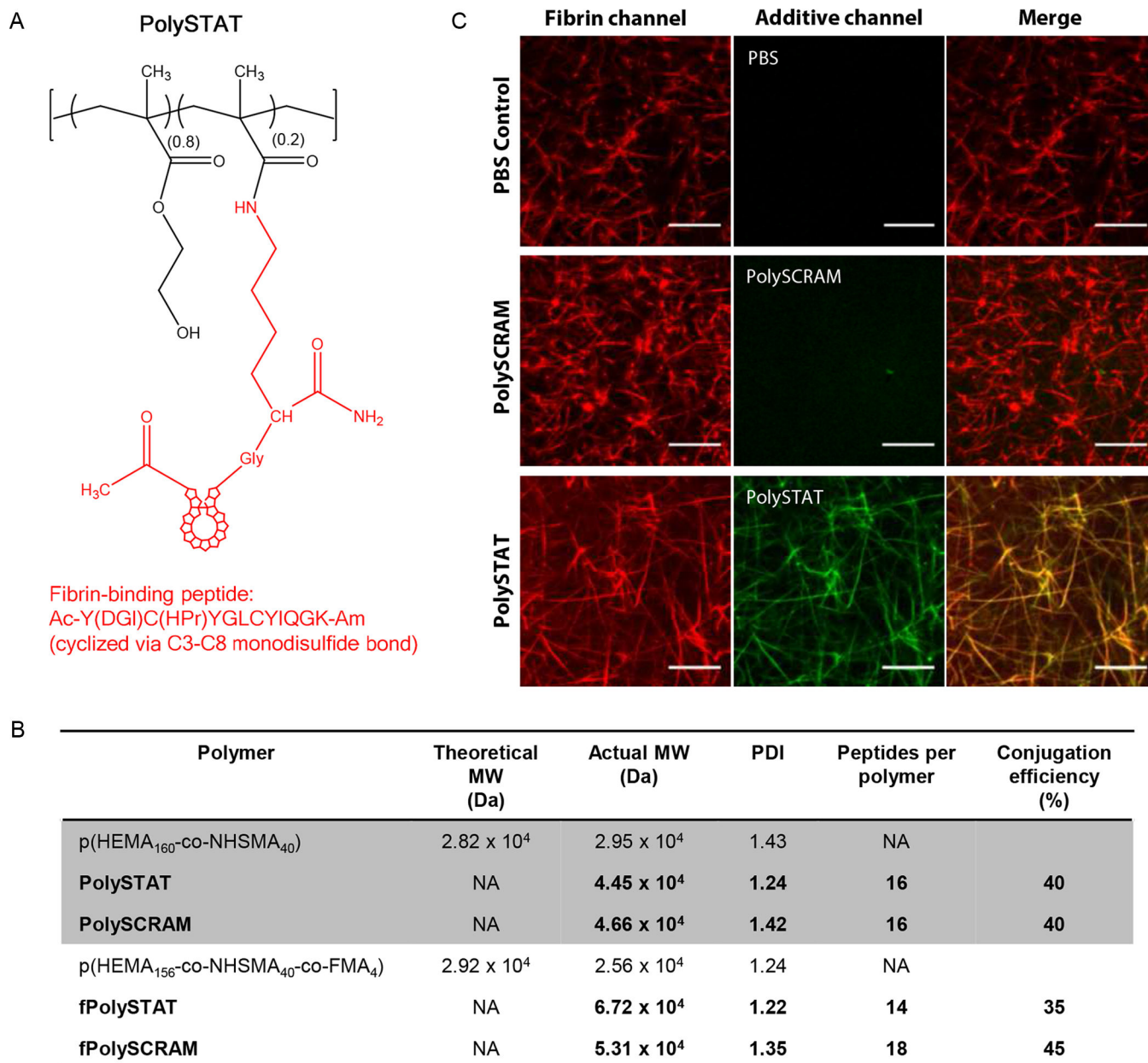


Fig. 1. PolySTAT synthesis and characterization

(A) The PolySTAT polymer backbone, a linear statistical copolymer of HEMA and NHSMA synthesized via RAFT polymerization, was grafted with the modified cyclic fibrin-binding peptide Ac-Y(DGI)C(HPr)YGLCYIQGK-Am (19) through NHS ester reaction with the lysine ϵ -amine. DGI, D-glutamic acid; HPr, hydroxyproline; Ac, acetylated N-terminus; Am, amidated C-terminus. (B) Two different polymer backbones were used, including a fluorescent fluorescein methacrylate (FMA)-modified p(HEMA-co-NHMA) for confocal studies. Polymer backbones were grafted with the fibrin-binding peptide for PolySTAT or a non-binding scrambled peptide for the PolySCRAM control. Actual molecular weight and polydispersity index (PDI) were determined using GPC. Peptides per polymer were calculated using UV absorbance. (C) PolySTAT integration into fibrin was confirmed using

confocal imaging. Pure fibrin clots were made using a solution of Alexa Fluor 546-labeled fibrinogen (red) and thrombin mixed with PBS, fPolySTAT (green), or fPolySCRAM (green). Scale bars, 10 μ m.

Author Manuscript

Author Manuscript

Author Manuscript

Author Manuscript

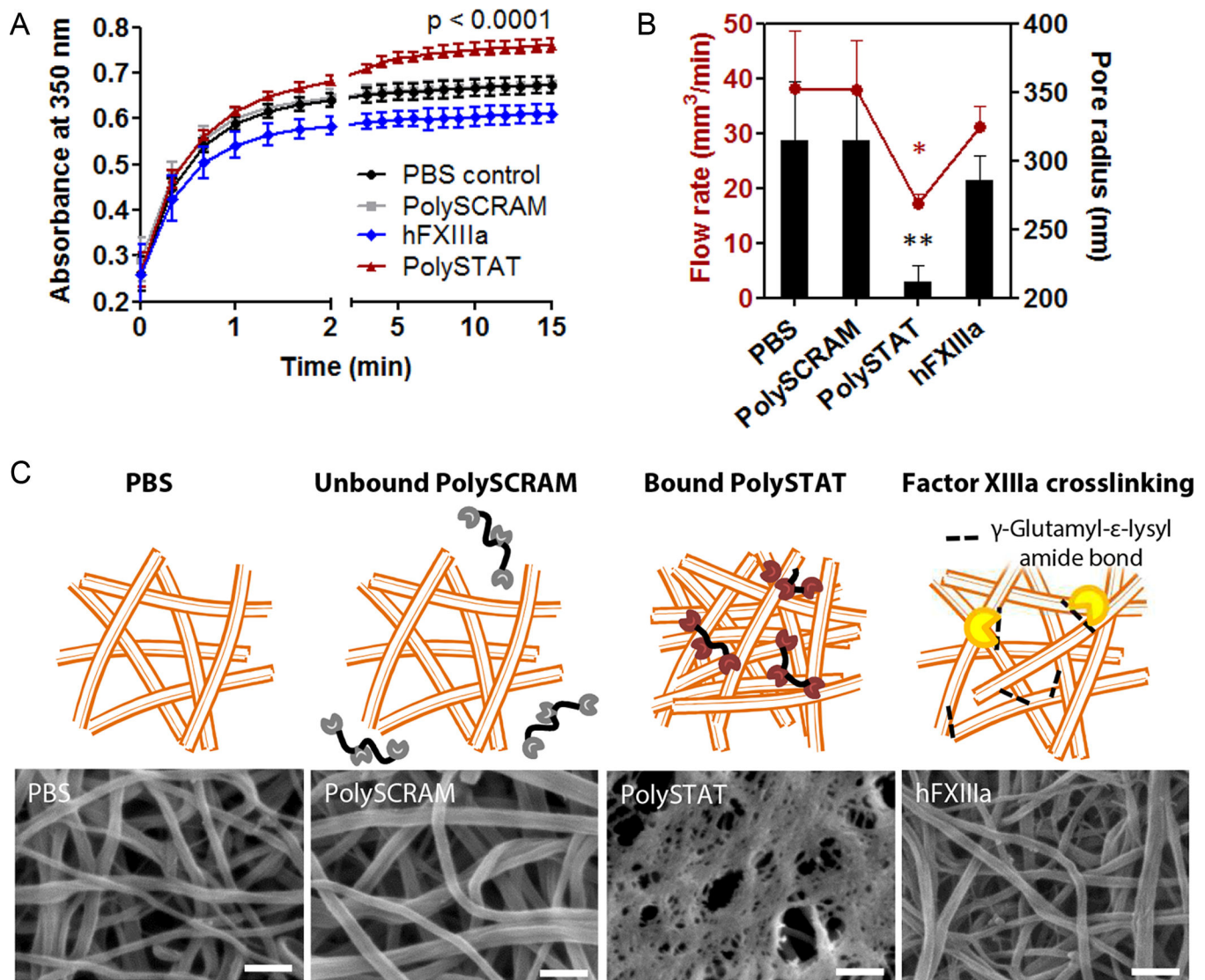


Fig. 2. *In vitro* characterization of PolySTAT-modified fibrin architecture

(A) Turbidity of pure fibrin clotting solutions with PBS, PolySCRAM, PolySTAT, and hFXIIIa was measured to determine if there were potential changes in fibrin nanostructure. The *p*-value shown is for comparison between PBS and PolySTAT at $t = 15$ min. (B) Flow rates of water through fully-formed fibrin were measured and used to extrapolate pore size using Darcy's Law and a model by Carr and Hardin (41). *P*-values are shown for comparison to PolySCRAM ($*p = 0.03$, $**p = 0.01$). Data in (A and B) are averages \pm SD ($n = 3$). Statistical significance was determined using one-way ANOVA with Tukey Kramer post hoc test. (C) Fully formed fibrin clots were imaged using scanning electron microscopy to visualize fibrin architecture. hFXIIIa was included for a crosslinking control. Scale bars, 250 nm. Schematics above the SEM images depict the exclusion of non-binding PolySCRAM from fibrin, PolySTAT-induced fibrin crosslinking via binding of fibrin-binding peptides, and enzymatic crosslinking by hFXIIIa. (Schematics are not drawn to scale.)

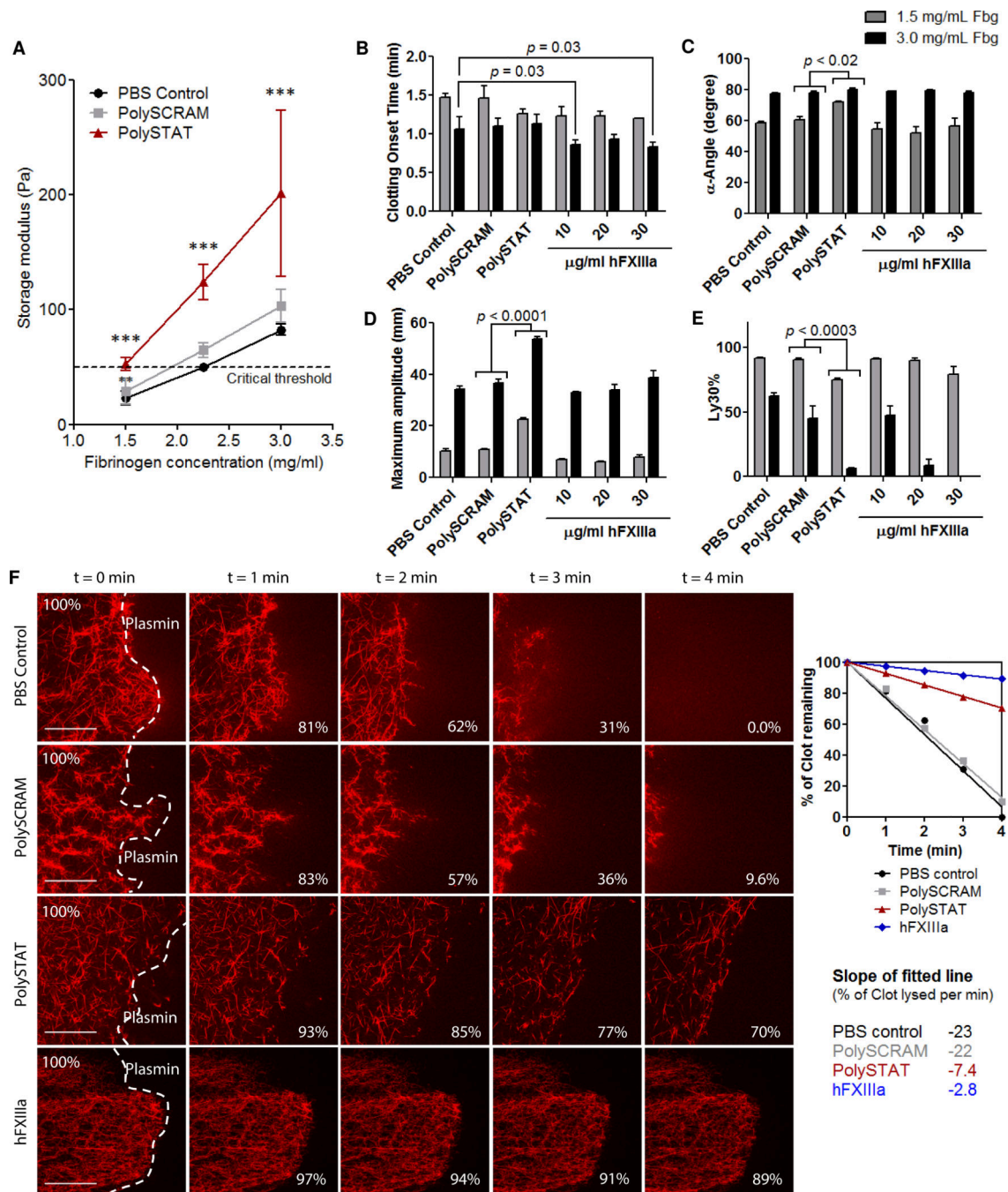


Fig. 3. In vitro characterization of fibrin polymerization kinetics, clot strength, and fibrinolysis (A) Cone-and-plate rheometry was used to measure PolySTAT-induced changes in fibrin storage moduli, a measure of elasticity. Measurements were taken for PolySTAT-modified and control fibrin formed with 1.5, 2.2, and 3.0 mg/ml fibrinogen with intact hFXIIIa ($n = 3$). The critical threshold indicates the storage moduli below which mortality increases dramatically in trauma patients (26). Data are averages \pm SD. *** $p < 0.0001$ for both effect of treatment and fibrinogen concentration, $p = 0.07$ for interaction; 2-way ANOVA. The effect of PolySTAT on clotting kinetics, clot strength, and extent of fibrinolysis was

evaluated in a hyperfibrinolytic model using TEG. (**B** to **E**) Clotting onset time, clotting rate, maximum clot strength, and extent of clot lysis 30 min after time to maximum clot strength are shown. Three hFXIIIa concentrations were included to compare to PolySTAT activity. Data are averages \pm SD ($n = 3$). *P*-values were determined using one-way ANOVA with Tukey Kramer post hoc test. (**F**) Lysis of fibrin was visualized using confocal microscopy. Plasmin (10 μ g/ml) was applied to the edge of fully-formed fibrin clots and time-lapsed images were taken. Image processing was used to measure the area of the clot in acquired images and determine rate of clot lysis. Scalebars, 50 μ m.

Author Manuscript

Author Manuscript

Author Manuscript

Author Manuscript

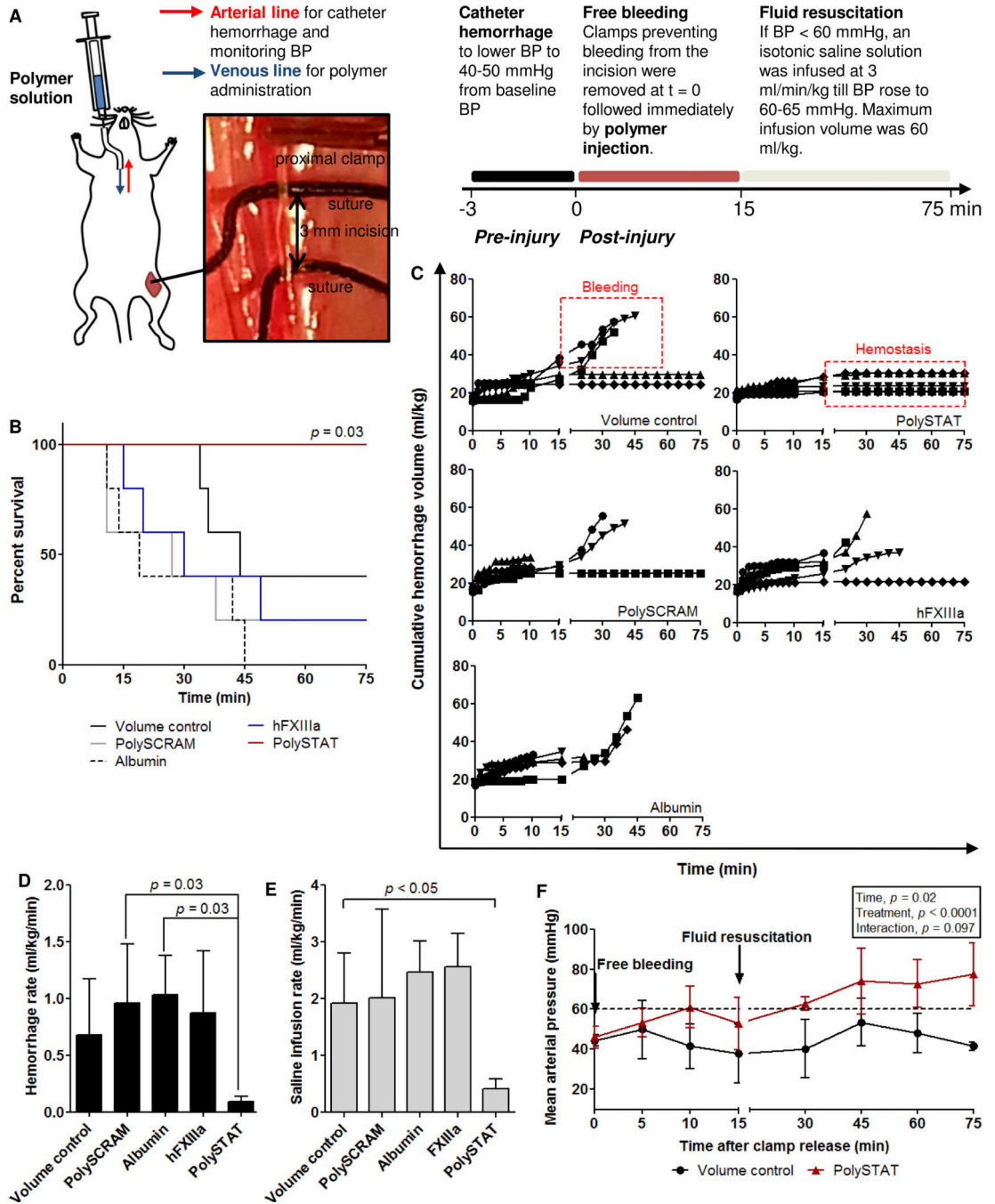


Fig. 4. Evaluation of PolySTAT in a rat model of femoral artery injury and fluid resuscitation (A) Workflow schematic. Rats were normalized to the same starting blood pressure, and clamps proximal and distal to the injured femoral artery were removed to allow the wound to bleed freely. Following clamp release, polymer solutions were injected. The wound was allowed to bleed or clot without interference for the first 15 min and subsequent challenge to the clot was presented in the form of 0.9% saline infusion to maintain BP above 60 mmHg for 60 min. (B) Survival of animals over the 75-min protocol (n = 5 per treatment). P-value determined using the log-rank Mantel-Cox test. (C) Bleeding profiles for volume controls

(Vol; 0.9% saline; top) and PolySTAT-treated animals (bottom) which are representative of clots that experience bleeding during fluid resuscitation and clots that maintain hemostasis during fluid resuscitation, respectively. Data are single measurements per timepoint, per animal (n = 5 per treatment group). **(D)** Cumulative blood loss normalized to survival time, including blood lost during catheter hemorrhage, the free bleeding period, and fluid resuscitation. **(E)** Saline infusion volumes normalized to survival time. Data in **(D and E)** are averages \pm SD. *P*-values were determined using a 1-way ANOVA and TukeyKramer post hoc test. **(F)** Mean arterial pressure was tracked over the protocol time to determine if animals were hypotensive. **(G)** Circulating lactate levels were measured to evaluate tissue perfusion. Data in **(F and G)** are averages \pm SD with variable n depending on survival times (11–75 min). A two-way ANOVA was used to determine the effect of time and treatment on MAP.

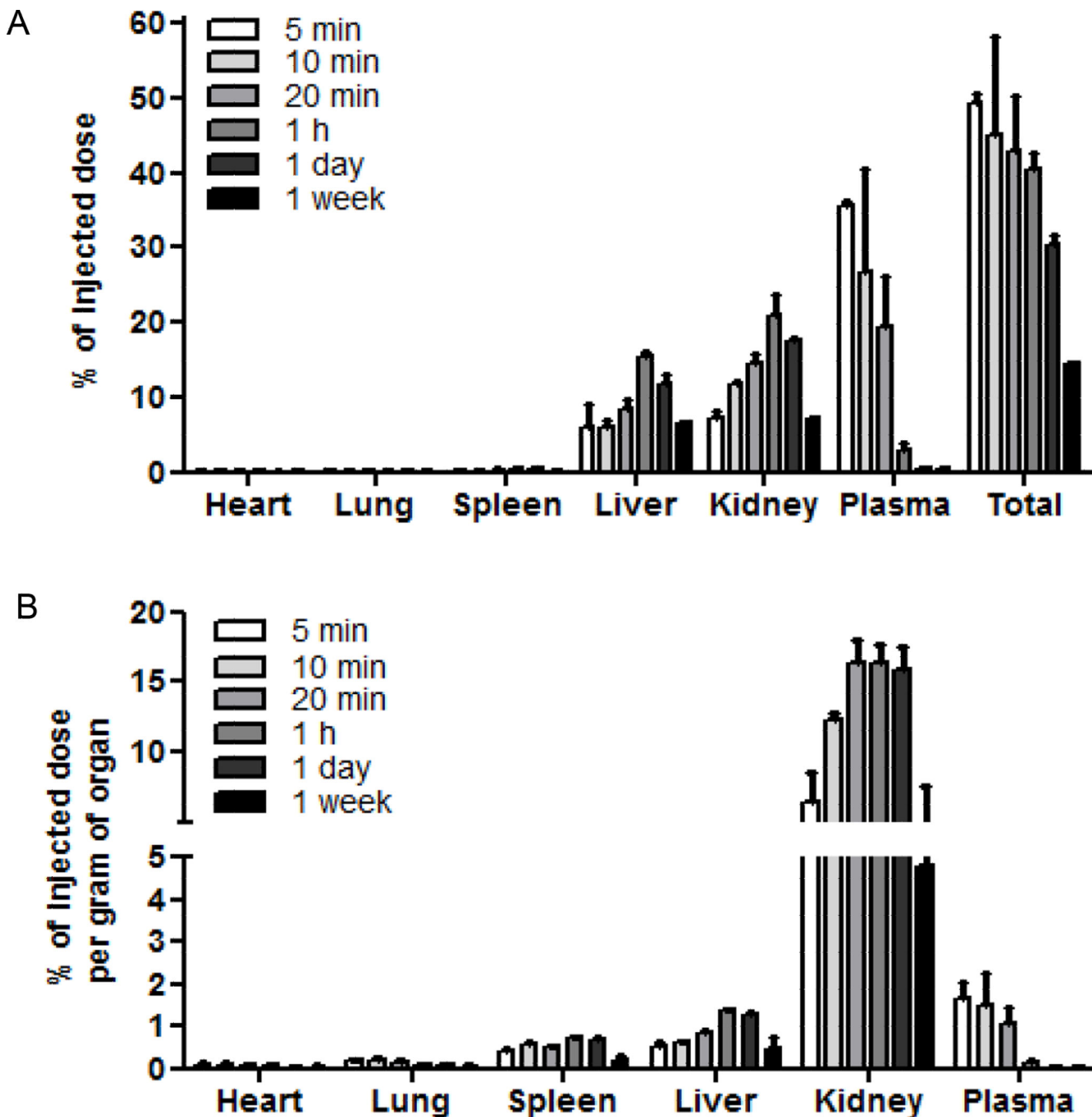


Fig. 5. PolySTAT biodistribution

PolySTAT was administered via tail-vein injection at a dose of 15 mg/kg in rats. Animals were euthanized at various time points to determine polymer biodistribution. **(A)** Percentage of the injected dose in whole organs at various timepoints. **(B)** Percentage of injected dose normalized to organ mass. Data are averages \pm SD ($n = 3$).